Free energy barriers to melting in atomic clusters

R. M. Lynden-Bell and D. J. Wales
University Chemical Laboratories, Lensfield Road, Cambridge CB2 1EW, United Kingdom

(Received 7 March 1994; accepted 4 April 1994)

We employ an order parameter approach to investigate melting in clusters bound by the Lennard-Jones potential containing 13, 55, and 147 atoms. We find well-defined Landau free energy barriers between solidlike and liquidlike states for the two larger clusters. A barrier is also revealed in an approximate analytical calculation using only information derived from the potential energy surface. For the two smaller clusters the order parameters are calculated for a large number of local minima. This helps us to interpret the Landau free energy calculations and to comment upon the suitability of the various order parameters for the cluster melting process. Systematic quenching offers us further insight into melting events for the 55-atom cluster. Finally, we elaborate further upon the relationships between S-bends and probability distributions in different ensembles.

I. INTRODUCTION

Clusters of atoms or molecules are both similar to and different from bulk material. They provide a useful way of increasing our understanding of phenomena in bulk materials and on surfaces as well as being of interest in their own right. As the number of atoms, N, in a cluster gets sufficiently large one expects to find that most atoms in the interior have essentially the same environment as in the bulk, while the same is true of surface atoms and a macroscopic surface. For small enough N this distinction is no longer possible and bulk phenomena may disappear. In fact, for N less than about 50 cluster properties often depend sensitively and irregularly upon N.

The main question that we address is the characterization of melting and freezing in a finite atomic cluster. What does one mean by distinct phases in a small system? In a bulk system different phases have different macroscopic properties. They correspond to different regions of the $3N$ dimensional configurational space of the system. The phase transition between bulk liquid and solid is first order with a free energy barrier between the phases. At the melting transition temperature the free energies of the two phases are equal and coexistence of solid and liquid in contact with each other is possible. Below this temperature the presence of a high free energy barrier may allow the existence of the liquid phase even though it is not the most stable form thermodynamically. In this state the supercooled liquid is said to be metastable.

Clusters containing small numbers (7–55) of atoms have been observed to fluctuate spontaneously between solidlike and liquidlike forms[1] on a nanosecond time scale in simulations. At low temperatures the clusters are ordered and can be described as solids although the structure is different from bulk material. At high temperatures the cluster is definitely disordered and can be described as liquidlike. For an intermediate range of temperatures the cluster takes up both forms, and, in a constant temperature calculation, is observed to fluctuate between them. The liquidlike phase may be distinguished by (a) increased mobility, (b) greater average potential energy at the same temperature (lower temperature at the same total energy in the microcanonical ensemble), and (c) a decrease in order as measured by an appropriate order parameter.

We propose that if an order parameter Q can be found such that the Landau free energy $F(Q)$ has two minima for a range of temperatures then two distinct phases can be identified and can be said to coexist. As the size of the cluster tends to infinity the free energy barrier between these minima is expected to increase and the phase transition tends to a first-order bulk phase transition. In Sec. II we shall define the Landau free energy and show that the criterion of a double minimum in $F(Q)$ is equivalent to the existence of two distinct maxima in the probability distribution $p(Q)$ of the order parameter Q in the canonical ensemble (bimodality).

The practical problem is to identify a suitable order parameter. It must be a smooth function of the $3N$ atomic coordinates so that if the order parameter of the system changes from Q_1 to Q_2 it passes through intermediate values. We have considered a number of possibilities and conclude that the best order parameter to use depends on the cluster size. We then find that there are double minima in the Landau free energy for clusters containing 55 and 147 Lennard-Jones atoms. We have also investigated the free energy barriers between the phases. The heights of these barriers determine the dynamical behavior of the clusters. Indeed the most marked differences between the phase transition in these clusters and in the bulk is that the free energy barrier in the canonical ensemble is low enough to be easily surmounted, while the size of the clusters is such that the whole cluster is involved in the transition.

Previous investigations of clusters in the microcanonical ensemble have shown an inflection (at low particle numbers) in the potential energy versus temperature curve, which becomes an S-bend at higher particle number.[1–4] This behavior is typical of systems with first-order phase changes. We shall discuss the relation of these observations to our findings. The thermodynamic and dynamic properties of a cluster are determined microscopically by the underlying potential energy surface. In order to understand the properties of the free energy that we find in simulations, we search for minima and transition states of this surface. We discuss how far the thermodynamic quantities that we measure can be related to

 0021-9606/94/101(2)/1460/17/$6.00

TABLE I. Order parameters in ideal configurations.

	Q_4	Q_6	W_4	W_6
fcc	0.191	0.575	−0.159	−0.013
hcp	0.097	0.485	0.134	−0.012
bcc	0.036	0.511	0.159	0.013
Simple cubic	0.764	0.354	0.159	0.013
Icosahedral(local)	0	0.6632	0	−0.170

these stationary points, extending the considerations that have been developed in previous work for Lennard-Jones,[5,6] potassium chloride,[7,8] and water clusters,[9,10] for example.

II. ORDER PARAMETERS AND FREE ENERGY

A. Order parameters

One order parameter which we have used is the total configurational or potential energy of the cluster, E_c. For the smaller clusters this proved to be as satisfactory as any other order parameter that we tried. We have also considered some orientational bond order parameters. We investigated the four parameters, Q_4, Q_6, W_4, and W_6[11–13] previously used for bulk systems. In order to construct these, "bonds" are drawn between all atoms nearer than a prescribed cutoff distance (we used 1.24 times the nearest-neighbor separation). The Q_L order parameters are made up of the square of sums of spherical harmonics for all N_b bonds in the cluster,

$$Q_L^2=\frac{4\pi}{N_b^2(2L+1)}\sum_m\left|\sum_{\text{bonds}}Y_{L,m}(\hat{\mathbf{r}}_{ij})\right|^2, \tag{1}$$

and are invariant under rotations, while the W_L functions are the third-order invariants

$$W_L=\sum_{m_1,m_2}\begin{pmatrix}L & L & L\\ -m_1 & -m_2 & m_1+m_2\end{pmatrix}\times\bar{Q}_{L,-m_1}\bar{Q}_{L,-m_2}\bar{Q}_{L,m_1+m_2}, \tag{2}$$

where

$$\bar{Q}_{L,m}=\frac{\Sigma_{\text{bonds}}Y_{L,m}(\hat{\mathbf{r}}_{ij})}{(\Sigma_m|\Sigma_{\text{bonds}}Y_{L,m}(\hat{\mathbf{r}}_{ij})|^2)^{1/2}}. \tag{3}$$

Table I (taken from Ref. 11) shows how these order parameters vary for different ideal space filling lattices (fcc, bcc, hcp, and simple cubic). The value given for an icosahedral arrangement is for the 12 bonds around the central atom in an icosahedral 13-atom cluster.

B. Statistical mechanics of clusters

Because clusters are small systems the distinction between different statistical mechanical ensembles is important, and observations in the different ensembles can show markedly different properties. The cluster has momentum and position coordinates and associated with these has kinetic energy, E_K and potential energy E_c. The statistical mechanics of a classical system is completely determined if the phase space densities of states $\Omega_c(E_c)$ and $\Omega_K(E_K)$ are known. $\Omega_c(E_c)dE_c$ is the volume of configuration space with potential energy between E_c and E_c+dE_c while $\Omega_K(E_K)$ is the corresponding volume of momentum space. We shall distinguish four different ensembles, the microcanonical ensemble, the isopotential ensemble, the isokinetic ensemble, and the canonical ensemble.

The microcanonical ensemble is one in which the total energy, E, of the cluster is fixed with

$$E=E_c+E_K \tag{4}$$

so that the microcanonical density of states is given by

$$\Omega(E)=\int_0^E\Omega_c(E-E_K)\Omega_K(E_K)dE_K, \tag{5}$$

where we have chosen the energy of the lowest minimum of the potential energy surface to be the energy zero. Energy may be exchanged between kinetic and potential forms and the probability distribution function for the kinetic energy in the microcanonical ensemble is given by

$$p_K(E_K)=\Omega_c(E-E_K)\Omega_K(E_K)/\Omega(E)=c(E)\Omega_c(E-E_K)E_K^{\kappa/2-1}, \tag{6}$$

where $c(E)$ is independent of E_K.

There are two additional points which must be considered in the context of an ensemble of clusters. First if we are discussing the statistical mechanics of the cluster of N particles we must exclude the parts of phase space in which particles have evaporated from the cluster when calculating Ω_c. Previous workers have usually achieved this by enclosing the cluster in a container. We prefer to define the phase space of the *bound* cluster, C_N, as the region of configuration space for which all N particles are connected either directly or indirectly in terms of a distance criterion. Second, it is convenient to separate the center-of-mass motion and the overall rotation to keep the internal energy of the cluster fixed. Thus the total number of degrees of freedom is $\kappa=3N-6$ for clusters with no center-of-mass motion and zero angular momentum. The effects of nonzero angular momentum are interesting in their own right,[14–16] but lie beyond the scope of the present paper.

In the microcanonical ensemble the connection between statistical mechanics and thermodynamics is given by

$$S=k\ \ln\ \Omega(E)$$

and

$$\beta=(kT)^{-1}=\left(\frac{\partial\ \ln\ \Omega(E)}{\partial E}\right)_{N,V}, \tag{7}$$

where V is the volume. In particular the caloric curve of a system which shows T as a function of E is informative. An example is shown in Fig. 1. The derivative of this curve is the specific heat.

The canonical ensemble is one in which the system is in equilibrium with a heat bath. This ensemble has the advantage that the properties of configuration and momentum space are separable. The connection with thermodynamics is given by

$$A=-kT\ \ln\ Z$$

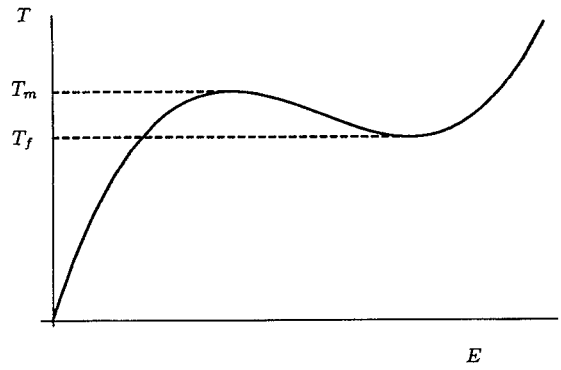

FIG. 1. Schematic microcanonical caloric curve exhibiting an S-bend, and definitions of the melting and freezing temperatures, T_m and T_f.

and

$$E=\left(\frac{\partial \ln Z}{\partial \beta}\right)_{N,V}, \tag{8}$$

where A and E are the Helmholtz free energy and the internal energy, respectively, $\beta=(kT)^{-1}$, and the canonical partition function, $Z(\beta)$, is the Laplace transform of the density of states $\Omega(E)$

$$Z=\int_{C_N} \exp[-E(\mathbf{r}_1,\ldots,\mathbf{r}_N,\mathbf{p}_1,\ldots,\mathbf{p}_N)/kT]d^{3N}r d^{3N}p$$

$$=\int_{C_N} \exp[-E/kT]\Omega(E)dE. \tag{9}$$

This integral is taken over all parts of phase space C_N which correspond to a bound cluster of N particles. In order to exclude the parts of phase space in which particles have evaporated from the cluster we define C_N as the region of configuration space for which all N atoms are connected either directly or indirectly employing a distance criterion. This is similar to the concept of an "intact cluster" considered by Stillinger and Stillinger.[17] In fact, the restriction in the second integral is contained in the definition of $\Omega(E)$ which is understood to be the total energy density of states for the bound cluster.

As the Laplace transform of a convolution integral such as Eq. (5) is a simple product we can separate the partition function into configuration and momentum terms

$$Z(\beta)=Z_c(\beta)Z_K(\beta),$$

where

$$Z_c(\beta)=\int_0^\infty \exp(-\beta E_c)\Omega_c(E_c)dE_c, \tag{10}$$

and the Helmholtz free energy is also the sum of configuration and momentum terms

$$A=A_c+A_K. \tag{11}$$

Again caloric curves can be constructed, but there is an important difference between the caloric curves of a canonical and a microcanonical ensemble in the coexistence region where the microcanonical ensemble can show an "S-bend" and the canonical ensemble cannot. An example of a caloric curve for a microcanonical ensemble is shown in Fig. 1.

The central part of the S-bend has a negative slope corresponding to a negative specific heat. Regions of negative specific heat are forbidden in canonical ensembles, but are allowed in microcanonical and isopotential ensembles of finite systems.[18] What is meant by a negative specific heat? If two such systems are brought into contact then, as expected, heat flows from the hotter to the colder system. But, as the specific heat is negative, this decreases the temperature of the colder system and increases that of the hotter system. Thus systems with negative specific heat are inherently unstable. In a canonical ensemble, where the system is in contact with an infinite heat bath, it is never found in a region of negative specific heat. The caloric curves for clusters in this ensemble show a point of inflection rather than an S bend.[19] In a bulk system as $N\rightarrow\infty$ this becomes a horizontal line joining the left-hand and right-hand branches of the curve. We should emphasize that, even in a microcanonical ensemble, S-bends only occur in finite systems. A uniform bulk system with a negative specific heat is unstable in the thermodynamic limit of large N and at constant energy as it can increase its entropy by splitting into two parts, each of which has a positive specific heat. Consequently, in this thermodynamic limit, results from canonical and microcanonical ensembles are the same. However, for finite systems, the interfacial region has a non-negligible entropy and free energy. As a result, the system may not be able to increase its entropy by splitting into two regions with positive specific heat.

The most marked difference between the phase transition in clusters and in the bulk is that the free energy barrier in the canonical ensemble is low enough to be easily surmounted, while the size of the clusters is such that the whole cluster is involved in the transition. Another way to think of this is in terms of the equilibrium constant between the two forms. For the bulk this is a step function of temperature, but for a cluster the step is smoothed out. As the cluster is warmed, melting is a gradual process, and one can define the melting temperature, T_m, as the highest temperature for which solidlike configurations are seen. This temperature is essentially the upper limit to the stability of the solid phase. Similarly a different (and lower) freezing temperature, T_f, can be defined below which the liquidlike configurations are no longer seen.[1,20–22] Thus phase coexistence in a cluster is revealed as the two phases coexisting at different times, rather than coexisting in contact. This finite size effect emphasizes the difference between the canonical and microcanonical ensembles. In the thermodynamic limit of an infinite bulk phase both ensembles give the same result, but in clusters the whole of the S-bend is accessible in a microcanonical calculation as the system is not big enough to fall into two parts, one solid and one liquid.

The isopotential and isokinetic ensembles are defined such that either the total potential energy or the total kinetic energy is fixed. Although neither are realizable in practice they can be achieved in simulations. The entropy and temperature of an isopotential ensemble (subscript c for configu-

rational) can be defined in a similar way to that of a microcanonical ensemble

$$S_c = k \ln \Omega_c(E_c),$$

and

$$\beta_c = (kT_c)^{-1} = \left(\frac{\partial \ln \Omega_c(E_c)}{\partial E_c} \right)_{N,V}. \tag{12}$$

In the coexistence region the isopotential caloric curves (T_c as a function of E_c) may show an S bend. We note that the necessary condition for the existence of an S bend in either the isopotential or the microcanonical caloric curve is equivalent to the condition that the corresponding entropy, $S_c = k \ln \Omega_c(E_c)$ or $S = k \ln \Omega(E)$ has two points of inflection,[23] i.e.,

$$\left(\frac{\partial^2 \ln \Omega_c(E_c)}{\partial E_c^2} \right) = 0$$

or

$$\left(\frac{\partial^2 \ln \Omega(E)}{\partial E^2} \right) = 0. \tag{13}$$

In this paper all our simulations are carried out in the canonical ensemble in which the temperature and number of particles are kept constant and the phase space is restricted to the bound cluster.

C. Free energy

There are two distinct free energies which we shall use in our discussion of clusters: the Helmholtz free energy, $A(T)$, and the Landau free energy $F(Q,T)$. The Helmholtz free energy of a classical system has already been defined in Eqs. (8) and (9) from which we see that the probability of finding the system with potential energy between E_c and $E_c + dE_c$ in a canonical ensemble at temperature T is given by

$$p_c(E_c;T)dE_c = \exp(-E_c/kT)\Omega_c(E_c)dE_c/Z_c. \tag{14}$$

The Landau free energy, $F(Q,T)$ is the free energy of the system for a particular value of the order parameter Q. The configurational part of the Helmholtz free energy, A_c, and the Landau free energy, F, are related by

$$\exp(-A_c/kT) = \int_{C_N} \exp[-F(Q,T)/kT]dQ \tag{15}$$

which follows from the definition of $F(Q,T)$:

$$\exp[-F(Q_0,T)/kT] = \int_{C_N} \exp[-E_c(\mathbf{r}_1,\ldots,\mathbf{r}_N)/kT]\delta(Q-Q_0)d^{3N}r, \tag{16}$$

where the integral is over all configurational coordinates. Since $F(Q,T)$ is generally calculated for particular temperatures we will henceforth drop the explicit T dependence. The previous equations show that

$$F(Q) = A_c - kT \ln p_Q(Q), \tag{17}$$

where $p_Q(Q)dQ$ is the probability of finding the system with values of Q between Q and $Q+dQ$, i.e., $p_Q(Q)$ is a (canonical) probability distribution function such that

$$p_Q(Q_0) = \int_{C_N} \exp(-E_c/kT)\delta(Q-Q_0)d^{3N}r/Z_c. \tag{18}$$

The most straightforward way of determining $F(Q)$ is just to sample the canonical distribution function at the appropriate temperature and use the resulting probabilities, $p_Q(Q)$, to construct $F(Q)$. This is the method that we employed for the 13 and 55 atom clusters. Molecular dynamics calculations were performed using a thermostat for sufficiently long times that both liquidlike and solidlike forms of the cluster were sampled.

In the 147 atom cluster, where high free energy barriers exist, this method is no longer practical as the simulated system does not explore both the solid and the liquid wells on the time scale accessible to simulation. Instead we bias the system[11,12] using a Q-dependent potential in such a way as to lower the free energy barrier. The probability $p_w(Q_0)$ of finding the biased system with the value of $Q = Q_0$ in the presence of the additional potential $w(Q)$ is then

$$p_w(Q_0) = \int_{C_N} \exp\{-[E_c(\mathbf{r}_1,\ldots,\mathbf{r}_N) + w(Q)]/kT\} \times \delta(Q-Q_0)d^{3N}r/Z_c(w), \tag{19}$$

where

$$Z_c(w) = \int_{C_N} \exp\{-[E_c(\mathbf{r}_1,\ldots,\mathbf{r}_N) + w(Q)]/kT\}d^{3N}r, \tag{20}$$

and hence

$$p_w(Q) = p_Q(Q)\exp[-w(Q)/kT]/Z_c(w). \tag{21}$$

Note that w can be taken out of the integral, whereas E_c cannot, because it has a unique value for a given Q. Equation (21) allows the probability $p_Q(Q)$ and hence the Landau free energy $F(Q)$ of the unbiased system to be determined. Details of the method are given elsewhere.[11,12] Umbrella sampling, in which small ranges of the appropriate order parameters are explored separately, was used with a Monte Carlo scheme for atomic displacements. An alternative approach has recently been investigated by Tsai and Jordan and Frantz *et al.*[10,24]

D. Interpretation of Landau free energy curves

Where the Landau free energy curve at a given temperature shows a double minimum it is also true that $p_Q(Q)$ is bimodal. In particular, if Q is the potential energy, E_c, then a double minimum in $F(E_c)$ implies the existence of an S-bend in the isopotential caloric curve. Equations (17) and (14) give (in reduced units)

$$F(E_c) = E_c - T \ln \Omega_c(E_c). \tag{22}$$

Differentiating this twice with respect to E_c we find

$$\left(\frac{\partial^2 F(E_c)}{\partial E_c^2}\right)_{N,T} = \frac{T}{T_c^2}\left(\frac{\partial T_c}{\partial E_c}\right)_{N,T}, \tag{23}$$

where T_c is the isopotential temperature. Hence a double minimum in $F(E_c)$ implies that the second derivative, and hence the slope of the isopotential caloric curve, changes sign twice.

We must now consider the physical meaning of the above result, and we focus upon the canonical ensemble. We identify the two minima with two distinct regions of phase space, corresponding to distinct phases. In these two regions the local minima of the potential energy surface correspond to solidlike and liquidlike conformations, respectively. The equilibrium constant in the canonical ensemble at temperature T is the ratio of the probabilities of finding the system in each region, which is given in terms of the Landau free energies as

$$K_{\rm eq}(T) = \frac{p(X;T)}{p(Y;T)} = \frac{\int_X \exp[-F(Q)/kT]dQ}{\int_Y \exp[-F(Q)/kT]dQ}, \tag{24}$$

where X and Y label the regions of order parameter space corresponding to the phases X and Y. We also associate the barrier in the Landau free energy with the actual barrier that must be overcome to move between the two phases or isomers. This assumes that an appropriate order parameter has been chosen.

The distinctness of the two (or possibly more) regions of phase phases depends on the height of the free energy barrier between them. If this is many times kT, fluctuations between the states are rare in the canonical ensemble and there is little ambiguity in determining which phase the system is currently in. This is the situation for bulk liquids and solids. As the free energy barrier becomes lower (as it is for the smaller clusters) the system fluctuates between phases and the possibility of identifying which phase the system is in depends on the time scale of the observation.[5,20,25,26]

There is a problem in choosing a suitable order parameter. In the work on bulk phases cited earlier[11,12] it was found that any of bond order parameters Q_6, Q_4, W_6, W_4 defined in Eqs. (1) and (3) were satisfactory. However, the lowest energy structures of the present clusters are all based upon icosahedra rather than fragments of a crystalline lattice, and we shall see in Sec. IV that the values of the bond-order parameters in liquid and solid phases of clusters are generally less distinct than in the bulk phases. Although we present some free energy results based on bond-order parameters, we found that the potential energy, E_c, provided a clearer distinction between the two phases in the 13 and 55 atom clusters, and most of the free energy curves shown employ the potential energy as the order parameter. The use of the potential energy also allowed us to construct entropy curves. For the 147 atom cluster we used a mixed order parameter $Q = E_c/100\epsilon + 4W_6$.

III. METHODS

A. Potential

The potential used was the Lennard-Jones two-body interaction where

$$\frac{E_c}{4\epsilon} = \sum_{\rm pairs}\left[\left(\frac{\sigma}{r_{ij}}\right)^{12} - \left(\frac{\sigma}{r_{ij}}\right)^{6}\right]. \tag{25}$$

No cutoff was applied in the simulations of 13 and 55 atom clusters; a cutoff of 3.9σ was used for the 147 atom cluster. Hereafter we may employ the abbreviation LJ_N for the Lennard-Jones cluster containing N atoms.

TABLE II. Details of the molecular dynamics runs.

Cluster	T^*	Run length/ns[a]	Evaporation events	Evaporation/ns
LJ_{55}	0.27	15	0	0
	0.29	20	24	1.4
	0.30	40	133	3.3
	0.31	17.6	110	6.3
	0.33	6	56	9.3
LJ_{13}	0.23	15	0	0
	0.19	15	28	1.9
	0.33	5.74	102	17.7

[a]After equilibration.

B. Sampling the canonical distribution

For clusters LJ_{13} and LJ_{55} simulations were carried out using molecular dynamics.[27] The velocity Verlet algorithm was used with a time step of 0.0196 reduced units (or 0.01 ps with atomic mass=39.95 amu, σ=3.4 Å, and ϵ/k_B=100 K). The clusters were thermostated by constraining the total kinetic energy to be constant. This generates an isokinetic ensemble, but as the kinetic degrees of freedom act as a heat bath for the configurational degrees of freedom, the distribution of configurational energies is the same as in a canonical ensemble.[28] The only unusual feature of the calculations was the restriction to geometries in which the clusters remained bound[17] [that is the restriction to the phase space C_N in Eq. (8)]. Whenever the order parameters were calculated (normally every 10 time steps) the configuration was tested to see whether any particles had evaporated. If so the trajectory was reversed for 100 steps, the velocities randomized, and the cluster equilibrated for a further 200 steps before continuing the averaging process. A spherical container has generally been used in previous work,[2,29,30] and we expect that our use of a bound cluster[17] should be equivalent to an appropriate container size, as determined by Tsai and Jordan.[10] Table II shows details of the runs.

C. Minima and transition state calculations

The probability distribution functions presented in Sec. V were calculated for samples of 1153 minima and 3481 transition states. The minima were found by systematic quenching from a high energy molecular dynamics trajectory.[31,32] Transition state searches and approximate steepest-descent rearrangement pathways were calculated by eigenvector-following as described elsewhere.[33] The new quench results described in Sec. V A were obtained in the same manner to investigate a particular melting event in greater detail. A statistical analysis of these results and the

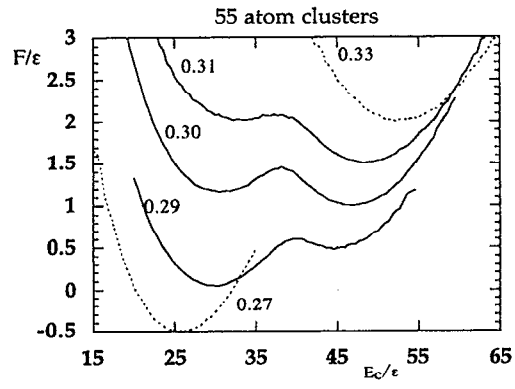

FIG. 2. Variation of the Landau free energy for LJ_{55} as a function of potential energy, E_c, at a number of temperatures. The values of the temperatures in reduced units are marked on the diagram. Note that the zero of free energy at each temperature is not determined and has been chosen arbitrarily.

properties of the reaction pathways, and a comparison with LJ_{19} and $(C_{60})_{55}$ clusters, is in preparation. Here we need only consider the probability distributions for the energies of the stationary points, and these were constructed by binning and smoothing.

IV. RESULTS

A. Free energy curves for clusters of 55 atoms

Our most thorough study has been of the cluster LJ_{55}. Figure 2 shows the variation of the Landau free energy as a function of potential energy, E_c, at a number of temperatures. Here, E_c is reported relative to the Mackay icosahedron[34] ($E_c=-279.248\,470\epsilon$). The two wells corresponding to solidlike and liquidlike forms are clearly seen. The solid well (with lower potential energy) is more favorable at $T^*=0.27$ and 0.29 while the liquid well is more favorable above $T^*=0.30$. The dotted curves correspond to temperatures at which no evidence of a second well was seen. The difference in the free energy of the wells varies rapidly with temperature, changing from $+0.45\epsilon$ to -0.52ϵ when the reduced temperature is changed by 0.02 between 0.29 and 0.31. The range of temperature over which there are both stable and metastable states, i.e., two minima, is small. At $T^*=0.27$ only the solid well is seen, while at $T^*=0.33$ only the liquid well is seen. This is in reasonable agreement with the isopotential ensemble calculations of Grimson[3] which show an S bend between reduced temperatures of 0.29 and 0.345 and with Stillinger and Stillinger.[17]

The barrier at coexistence, when the two forms have the same free energy, can be estimated from the run at $T^*=0.30$ and is approximately 0.45ϵ. We shall discuss later why this is probably a lower limit.

We found that surprisingly long runs were needed to sample both solidlike and liquidlike regions of phase space. Figure 3 shows trajectories from a 40 ns run at $T^*=0.3$. Even here it is not clear that the sampling is uniform. Another check is provided by looking at the configurational density of states Ω_c which should be independent of temperature. Plots of $\ln \Omega_c$ vs E_c are steep, approximately linear, functions of E_c. In order to emphasize the nonlinear variations in the density of states we subtract a linear term to define a new function Φ,

$$\Phi(E_c)=\ln \Omega_c(E_c)-E_c/T_{\mathrm{ref}}+A_c(T)/T, \tag{26}$$

which is constructed from the observed probabilities by [see Eq. (14)]

$$\Phi(E_c)=\ln p_c(E_c;T)+E_c(1/T-1/T_{\mathrm{ref}}). \tag{27}$$

The choice of the value of T_{ref} in the definition of Φ is arbitrary. The value 0.2982 was chosen to make the two maxima in the curve equal, and we shall show that this implies that the coexistence temperature in the canonical ensemble is equal to 0.2982.

There is good agreement between the curves for Φ in Fig. 4 at the five different temperatures investigated, showing that the runs are long enough for the configurational space to have been reasonably accurately sampled. The offset of the curves for different temperatures is due to variations in the last term in Eq. (26).

Once $\ln \Omega_c(E_c)$ or, equivalently $\Phi(E_c)$, is known then all the thermodynamical properties of the cluster may be calculated. The double maximum in these curves, which agrees with previous calculations,[2,29] emphasizes the presence of

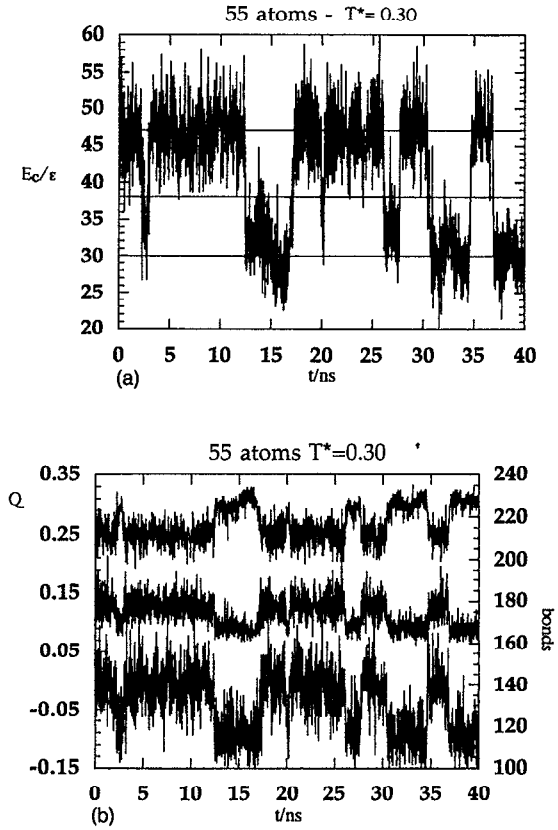

FIG. 3. Trajectories from the 40 ns run at $T^*=0.3$. (a) Potential energy; the horizontal lines correspond to maxima and minima of the free energy curve (see Fig. 5). (b) Top to bottom: number of bonds (defined by a distance criterion), $2Q_4+0.05$ and W_6. The right-hand scale is for the bond number and the left-hand scale is for the order parameters.

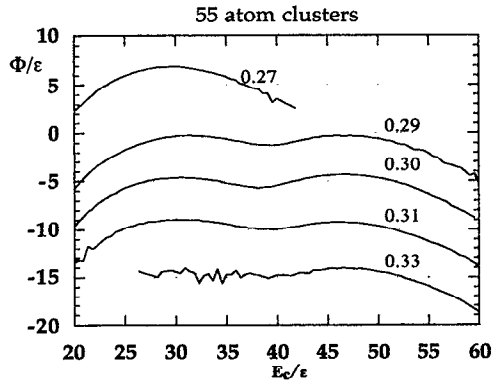

FIG. 4. Plots of Φ against E_c for LJ_{55} at a number of temperatures as marked. Φ is defined in the text, and is related to the configurational entropy, S_c.

points of inflection in the isopotential entropy $[S_c = k \ln \Omega(E_c)]$ as a function of E_c. We now show that the presence of such points of inflection implies both the existence of S-bends in the isopotential caloric curves and bimodality in the canonical potential energy distribution functions. Then we shall show that the canonical coexistence temperature can be determined by constructing the common tangent to either $\Phi(E_c)$ or $\ln \Omega_c(E_c)$.

The slope of the curves of $\Phi(E_c)$ is related to the inverse temperature of the isopotential ensemble by

$$d\Phi/dE_c = T_c^{-1} - T_{\mathrm{ref}}^{-1}. \tag{28}$$

Since $d^2\Phi/dE_c^2 = -(\partial T_c/\partial E_c)/T_c^2$ the condition for an S-bend in the isopotential caloric curve, $T_c(E_c)$, is that $\Phi(E_c)$ has two points of inflection. The first point of inflection corresponds to a local maximum in $T_c(E_c)$ and the second to a local minimum, as expected from Fig. 1. The intermediate point of maximum curvature in $\Phi(E_c)$ corresponds to the inflection point of $T_c(E_c)$ between the two turning points.

In order to find the condition for bimodality we recall that the probability distribution function for the potential energy, E_c, in a canonical ensemble at temperature T is

$$p_c(E_c;T) = \Omega_c(E_c) e^{-E_c/T}/Z_c(T). \tag{29}$$

(Note that we are using units for T in which Boltzmann's constant is equal to one). Taking logarithms and differentiating we obtain

$$\frac{\partial \ln p_c(E_c;T)}{\partial E_c} = \frac{\partial \ln \Omega_c(E_c)}{\partial E_c} - T^{-1} = T_c^{-1} - T^{-1} \tag{30}$$

and

$$\frac{\partial^2 \ln \Omega_c(E_c)}{\partial E_c^2} = \frac{\partial^2 \ln p_c(E_c;T)}{\partial E_c^2} = \frac{\partial^2 \Phi(E_c)}{\partial E_c^2}. \tag{31}$$

From Eq. (30) we see that the maxima and minima in the canonical distribution function at a given temperature, T, are determined by $T_c(E_c) = T$. The value of $T_c(E_c)$ is determined by the slope of $\Phi(E_c)$ using Eq. (28), and as, if the distribution is bimodal, $\ln p_c(E_c;T)$ has two maxima and an intervening minimum, there must be three values of the potential energy, E_c, where Φ has the same slope for bimodality to be possible. Points with the same slope cannot occur unless Φ has two points of inflection. The temperatures $T_{c,\min}$ and $T_{c,\max}$ determined from the slope of Φ at these two inflection points determine the range of temperatures over which the canonical distribution of potential energies is bimodal.

As we have already concluded that the condition for the existence of an S-bend in the isopotential ensemble is that Φ (or equivalently $\ln \Omega_c$) has two points of inflection, we deduce that the existence of bimodality in $p_c(E_c;T)$ for some finite range of T is a necessary and sufficient condition for the presence of an S-bend in the isopotential caloric curve. Similarly the presence of an S-bend in the isopotential caloric curve implies that there is a range of temperatures over which the canonical distribution function is bimodal. An analogous argument leads to the conclusion that bimodality in the canonical distribution of the total energy implies the existence of an S-bend in the microcanonical caloric curve and vice versa.[23]

We now define the coexistence temperature in the canonical ensemble using a common tangent construction. If it is possible to draw a straight line that is a tangent to $\Phi(E_c)$ at two energies, E_{c1} and E_{c2}, then, from the preceding argument, these correspond to maxima in the canonical probability distribution function at a temperature determined by the slope of the common tangent $m = (T^{-1} - T_{\mathrm{ref}}^{-1})$. Because they lie on a common tangent, these maxima are equally probable as, from Eq. (27)

$$\ln p_c(E_{c1};T) - \ln p_c(E_{c2};T) = \Phi(E_{c1}) - \Phi(E_{c2}) - (E_{c1} - E_{c2})(T^{-1} - T_{\mathrm{ref}}^{-1}), \tag{32}$$

which vanishes as the two points lie on the same straight line with gradient $(T^{-1} - T_{\mathrm{ref}}^{-1})$. We define the temperature, T, determined from the slope of the common tangent, as the coexistence temperature.

We note that other definitions of the coexistence temperature are possible. In our definition the maxima in the probability distribution functions are equal, $p_c(E_{c1};T) = p_c(E_{c2};T)$, but the total probabilities of finding the system in configurational energies corresponding to the two phases, X and Y, are not necessarily the same. For example, if we model the two peaks in $p_c(E_c;T)$ by Gaussians then the integrated probabilities of these peaks should provide some idea of the relative probability:

$$p_X/p_Y = \sqrt{C_Y/C_X}, \tag{33}$$

where $C_X \propto [\partial^2 \ln p_c(E_c;T)/\partial E_c^2]_{E_c = E_{c1}}$ is the heat capacity associated with the X phase (the first derivative evaluated at E_{c1} vanishes). In practice the temperature at which the total probabilities are equal is likely to be very close to our coexistence temperature.

The canonical temperature at which a common tangent might exist for the microcanonical entropy $[\partial \ln \Omega(E)/\partial E]$ as a function of the total energy E need not be exactly the same as for the isopotential ensemble. However, we can argue that the microcanonical and isopotential caloric curves will generally exhibit the same features. The probability dis-

tributions for the configurational, kinetic and total energy in the canonical ensemble are related by the convolution

$$p(E;T)=\int_0^E p_c(E-E_K;T)p_K(E_K;T)dE_K$$

$$=\int_0^E p_c(E-E_K;T)\,\frac{E_K^{\kappa/2-1}e^{-\beta E_K}}{\beta^{\kappa/2}\Gamma(\kappa/2)}\,dE_K, \qquad (34)$$

where Γ is the Gamma function. The probability distribution for the kinetic energy, $p_K(E_K;T)$, has a single maximum at $E_K=(\kappa/2-1)kT$ which becomes broader as κ increases. Differentiation with respect to E gives

$$p'(E;T)=\int_0^E p_c'(E-E_K;T)p_K(E_K;T)dE_K. \qquad (35)$$

Unless the probability distribution function for the potential energy has two maxima, so that $p_c'(E_c;T)$ has three zeros as a function of E_c, $p'(E;T)$ will have a single zero. In general the convolution of an objective function with a smooth function that has a single peak, such as $p_K(E_K;T)$, smears out the structure in the objective function. Thus if $p_c'(E_c;T)$ has three zeros [i.e., $p_c(E_c;T)$ has two maxima] then $p'(E;T)$ will also have three zeros if the maximum in $p_K(E_K;T)$ is sharp enough, but will lose them if it is too broad. We therefore deduce that the S-bend in the microcanonical caloric curve will be less pronounced than for the isopotential ensemble. Furthermore, the existence of the isopotential S-bend is a necessary, but not sufficient, condition for the presence of the microcanonical S-bend.

As stated previously, the reference temperature of 0.2982 used in the definition of Φ was chosen to make the common tangent to $\ln \Omega_c(E_c)$ horizontal (within the error of the numerical experiments) and gives the value of the coexistence temperature as $T=0.2982\pm0.002$. Such bimodality has been previously observed around $T^*=0.3$ in both simulations[2] and theory.[29]

The presence of an S-bend in the caloric curve of the isopotential ensemble and of an inflection in that of the canonical ensemble can be understood qualitatively from the curves in Fig. 4. As the potential energy is increased from zero the slope initially decreases corresponding to a steadily increasing temperature in the isopotential ensemble. At the first maximum in Φ the temperature is equal to 0.298, and it continues to increase until the point of inflection is reached. Then between the first and second points of inflection on either side of the minimum the temperature *decreases* as the energy increases. This is the region of the S-bend where the isopotential specific heat is negative. After the second point of inflection the specific heat becomes positive again and the temperature continues to increase as the potential energy is increased. In the canonical ensemble the specific heat is necessarily positive as it is proportional to the square root of the mean square energy fluctuation.

Because the clusters have rather few degrees of freedom, the free energy wells are fairly broad, so that the system can be found with a range of potential energy around the minima for each well. The values of the potential energies in the two

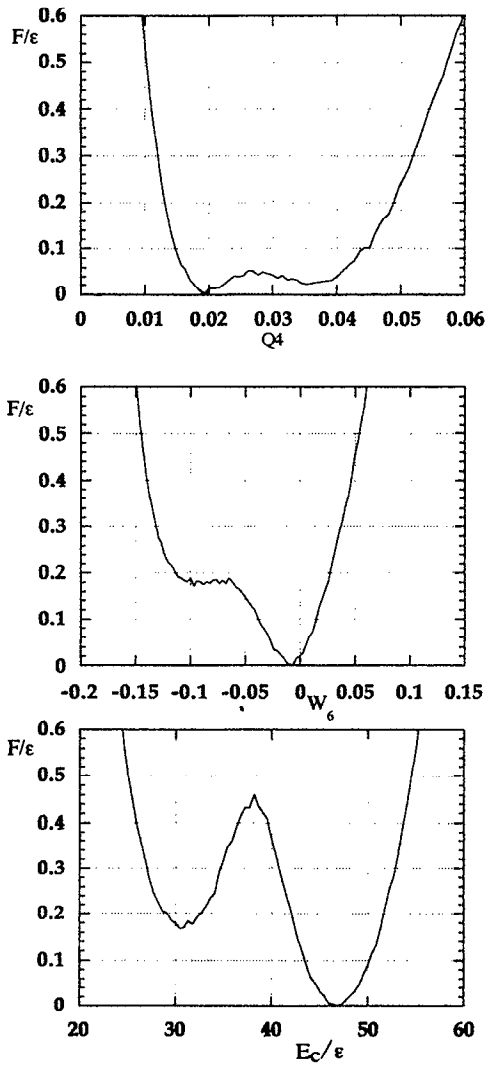

FIG. 5. Free energy curves calculated for a number of different order parameters at $T^*=0.3$. Top: Q_4; middle: W_6; bottom E_c/ϵ. In each case the zero of free energy has been chosen at the bottom of the solid well. For Q_4 the solid well corresponds to low Q_4.

minima are approximately $E_c=30\epsilon$ and $E_c=47\epsilon$ for solidlike and liquidlike phases, respectively, at the coexistence temperature.

How reliable are these results? Although the above argument suggests that the runs are long enough to sample configurational space satisfactorily it is not clear that the free energy barriers are accurate. Figure 5 shows free energy curves calculated for a number of different order parameters at $T^*=0.3$. The bond-order parameter Q_6 (not illustrated) has a single well while Q_4 and the triple bond invariant W_6 do not show a clear free energy maximum. The reason that the results for these other order parameters do not discriminate between solid and liquid states of these clusters, although they do for bulk phases, is that the spread of values in the two states overlaps. We shall discuss this further in Sec. V. Given that the bond order parameters do not discriminate between the states we should ask whether the potential energy, E_c, performs better. The horizontal line in Fig. 3(a)

corresponds to the value of E_c at the maximum in the free energy curve. There are some fluctuations in both solid and liquid phases which cross this line showing that it is not an ideal discriminator. We conclude that the size of the barrier estimated from the curves in figure 2 is a lower limit. If the number of crossings at this maximum is twice the number of true transitions we conclude that the free energy barrier is underestimated by 0.20ϵ. This follows because if the probability p_Q in Eq. (17) is doubled, the apparent value of $F(Q)$ is decreased by about 0.2ϵ at $T^*=0.3$.

The double minimum in the Landau free energy should be contrasted with the bimodality exhibited by the short time averaged temperature in the microcanonical ensemble. The temperature between the two peaks is rarely sampled and corresponds to an average between the two wells for a segment of trajectory that passes between them.[6] The intermediate value of E_c for the barrier region of the Landau free energy curve does not correspond to an average between the two minima because the curve is constructed from instantaneous rather than short time averaged quantities. However, a time averaged quantity would present new problems as an order parameter because it is not a function of the instantaneous position in phase space.

V. ORDER PARAMETERS AND THE POTENTIAL ENERGY SURFACE

A. Qualitative correlations and quench results

Figure 6 shows the probability distribution functions found for the potential energy of minima and transition states of LJ_{55} which were obtained from a high energy molecular dynamics trajectory as described in Sec. III C. The solid lines show the distribution of minima on the potential energy surface. The global minimum at $E_c=0$ corresponds to a structure with icosahedral symmetry (Mackay icosahedron).[34] As the energy increases there are first small numbers of minima which correspond to defective icosahedral structures, for example with single and double cap-defect pairs in the surface.[17,35] Finally, at about $E_c=15\epsilon$ above the icosahedron there are large numbers of minima which generally have disordered structures.

The dashed lines in Fig. 6 show the probability distribution of transition states. In Fig. 6(a) the two distributions are referred to a common energy zero. We note from Fig. 6(b) that when the transition state distribution is referred to an energy zero at the lowest transition state, rather than the global minimum, features at low energy in the two distributions coincide.

The difference between a solid and a liquid can be related to the potential energy surface. The solid has a single low energy minimum and at low temperatures the system is confined to the region of phase space around this minimum. The entropy is low because the volume of accessible phase space is small. Atomic mobility is also low as the probability of reaching other regions of phase space is extremely small. In the liquid phase the system has enough potential energy to reach regions of phase space associated with the minima at higher energies. As there are many of these, the system has a greatly increased volume of accessible phase space and hence greater entropy. The atomic mobility is also much higher as all the many potential minima are associated with different structures.

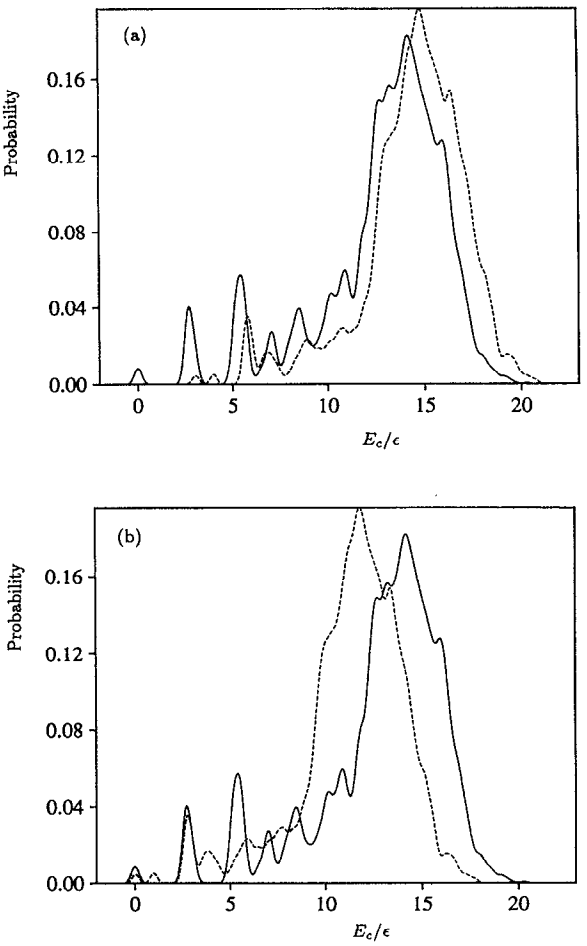

FIG. 6. Probability distribution functions for the potential energy of minima (solid lines) and transition states (dashed lines) of LJ_{55}. Because of the finite samples of data points these curves will be least reliable at higher potential energy. (a) A common energy zero is chosen for both distributions corresponding to the global minimum. (b) The energy zero for the transition state distribution is taken as the lowest energy transition state.

This description of the liquid depends on the transition states between the various minima being low enough that the system can move over a large volume of phase space. If this were not true one would have a glass rather than a liquid.

In order to relate the distribution of potential energy minima to the free energy one must remember that the potential energy of a system at finite temperature is almost always higher than that of the nearest minimum (see Fig. 7). In a harmonic system with κ vibrational normal modes one expects an average potential energy roughly equal to $\kappa kT/2$ above the minimum potential energy, i.e., half the equipartition energy for κ vibrational modes. For 55 atoms at the coexistence temperature this is about 25ϵ which would suggest an energy of roughly $25-30\epsilon$ for the solid well and 40ϵ for the liquid well, a little lower than we actually observe. These average energies are well in excess of the lowest re-

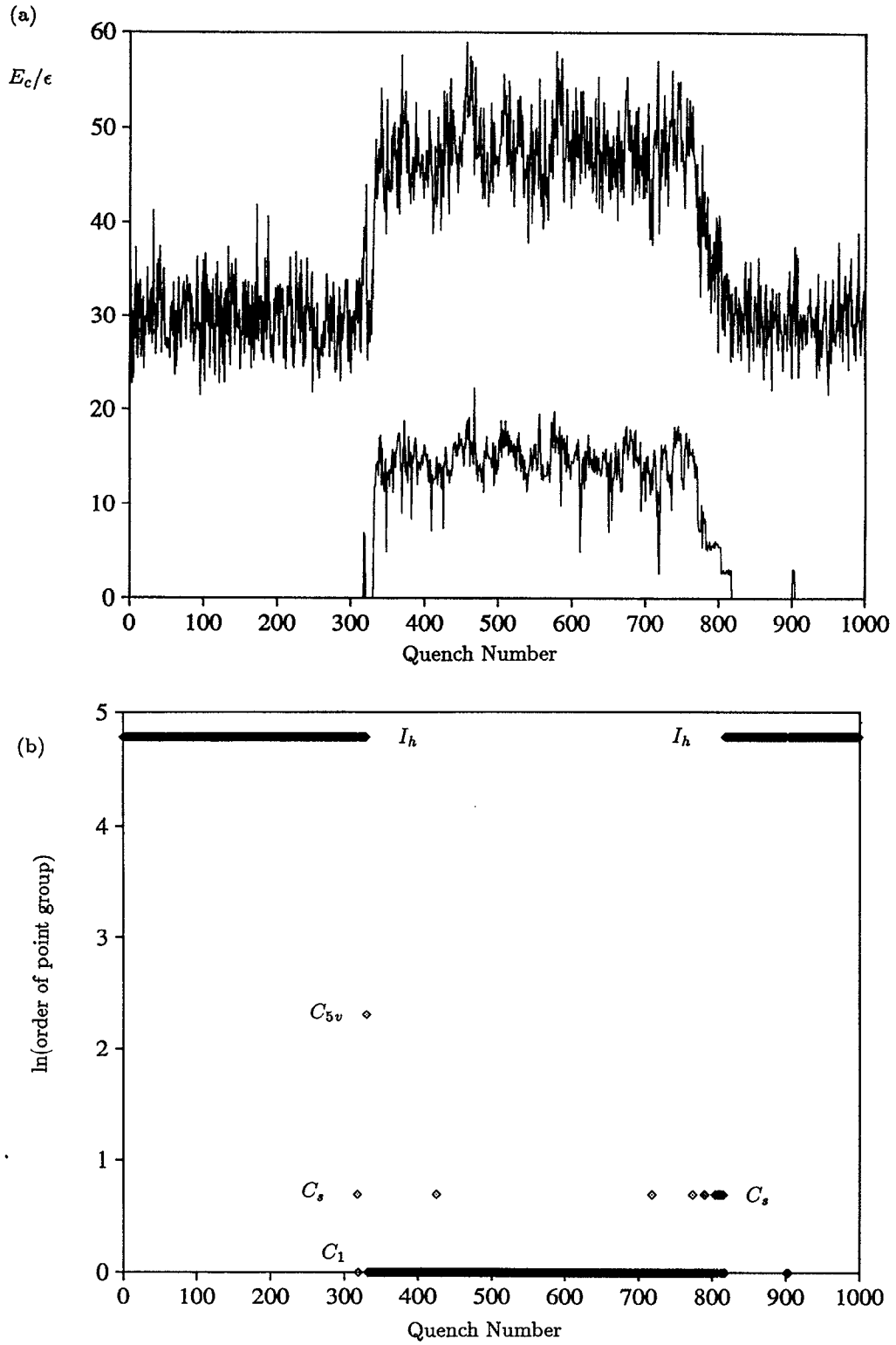

FIG. 7. (a) Potential energies relative to the global minimum of 1000 configurations (upper curve) and the minima that they quench to (lower curve) from a trajectory segment of length 4 ns at $T^*=0.3$ that shows a melting and a freezing event. (b) Orders of the point groups of the quench minima. The logarithm is taken to provide a more convenient range.

arrangement barriers.[35] The probability distribution function calculated for a sample of 3481 transition LJ_{55} states shows a large increase at about $E_c=12\epsilon$ which presumably contains the pathways between solidlike and liquidlike states, rather than between minima based upon underlying icosahedral order. This means that the transition states are readily accessible from the liquid and solid at coexistence, justifying our identification of the free energy maximum at an intermediate

value of E_c as the "Landau transition state" for the solid to liquid transition.

To gain further insight into the melting process we have employed systematic quenching along a particular trajectory near the coexistence temperature. This technique, introduced by Weber and Stillinger,[31,32] associates any instantaneous configuration with a unique local minimum on the potential energy surface by steepest-descent energy minimization. In the present work eigenvector-following minimization was employed[33] which will generally give the same results as true steepest-descent quenching, although we note that the boundaries between multidimensional basins of attraction may be very complicated.[36] The resulting time-ordered series of minima represents the melting process as a series of transitions between well-defined topological regions of the surface. Stillinger and Stillinger[17] have previously applied the method to a model 55-atom inert gas cluster to good effect.

In the present case 1000 quenches were performed at intervals equivalent to 4 ps for the Lennard-Jones parameters given in Sec. III B. The segment of trajectory in question contains both a melting and a freezing transition. This is evident from Fig. 7(a) where the configurational energy at the start and finish of each quench is plotted against the quench number. In agreement with Stillinger and Stillinger[17] we find that the solidlike regions of the trajectory are associated almost entirely with a single structure, namely the global minimum icosahedron. The liquidlike regions are associated with many different disordered structures that have potential energies drawn from the major peak of the probability distribution shown in Fig. 6. These observations are further reinforced by Fig. 7(b), which shows the variation of the order of the point groups found for the quench minima in the same order. The logarithm has been plotted to show the lower symmetry minima more clearly. As expected, the high energy minima in the liquidlike region generally have C_1 symmetry.

Examination of about half a dozen individual crossings between solid and liquid phases of the 55 atom cluster at $T^*=0.3$ showed no evidence that the system had to pass through a configuration with potential energy to the right of the liquid well in the free energy curve before making the transition. However, the potential energy was generally found to be higher in the liquid than in the transition region. This shows how the finite temperature and interconversion of kinetic and potential energy obscure the rearrangement mechanism on the potential energy surface. For example, at the transition between the solid and liquid phases in Fig. 7 we find that consecutive quenches arrive at the I_h global minimum and a structure with C_{5v} symmetry. This sequence was also observed when the quench interval was reduced by a factor of 5. Hence we searched for a rearrangement between the two structures in question. A direct interconversion was not found, (which does not necessarily mean that it does not exist) but we did find a two-step process which achieves the same effect. The intermediate minimum has C_5 symmetry as do both transition states—one of the C_5 axes is maintained throughout (Fig. 8). Note that the potential energy of these transition states is lower than the average potential energy of the liquid minima.

B. Bond-order parameters

Figures 9(a)–9(d) give scatter plots of order parameters defined by Eqs. (1) and (3) vs potential energy for local minima of LJ_{55}. It should be remembered that these order parameters are global in the sense that they are related to the sums of properties of all the bonds in a cluster. Figure 9(d) is the best one to start with. The global minimum has the most negative value of W_6. The defective structures and the disordered structures, particularly, have larger values of W_6.

Let us compare this to what we might see for bulk material. First one would expect to find a single low energy minimum corresponding to the crystalline phase which has a highly ordered structure. Then one would expect an energy gap followed by many minima which have a spread of energies, but no long range order. For these minima W_6 (or any other global bond-order parameter) would be equal to zero. One would also expect a few minima corresponding to defective solid structures with nonzero values of the order parameters.

Now returning to Fig. 9, we see that at least Fig. 9(d) shows the expected behavior. Because the cluster is small, and even in a bulk liquid there is a good deal of local order, it is not surprising that the minima do not have order parameters which are exactly zero, although the values of W_6 do get closer to zero for the higher energy minima. The other order parameters behave in a more unexpected way. The mean value of Q_6 remains roughly constant as the energy increases, values of W_4 scatter widely at all energies investigated, while the mean value of Q_4 actually increases with increasing energy. These unexpected results are due to the preference for icosahedral symmetry (for which Q_4 and W_4 are equal to zero, see Table I) and to the small size of the clusters which allows order in the liquidlike phases. Furthermore, the values calculated for the icosahedron can be extremely sensitive to how well converged the structure is, showing that these order parameters can vary pathologically around this structure.

These results can be used to interpret the values observed in the simulations (see Table III). In bulk phases the distinction between an ordered solid in which the order parameters are nonzero and a liquid or glass in which they vanish is clear. Even in simulations of a few hundred atoms with periodic boundaries the liquid state parameters are close to zero. Clusters are a different matter. As shown in Table III, even in the high temperature states, which we have described as liquid Q_4 and Q_6, are not equal to zero. Indeed the value of Q_4 increases with temperature in all three cluster sizes, while Q_6 increases in the 13 atom cluster and only gradually approaches zero in the disordered states as N increases from 13 through 55 to 147.

The most interesting order parameter for these clusters is W_6. In all three clusters this order parameter is large and negative for the icosahedral global minimum with a value extremely close to that for 13 atoms. This value is typical of icosahedral symmetry. Other structures such as fcc, hcp, and bcc have magnitudes of this order parameter less than one-tenth of this value in the ideal lattices. As the temperature is raised in the 55 and 147 atom clusters the magnitude of W_6 decreases and in the liquid state it tends to zero. This is what

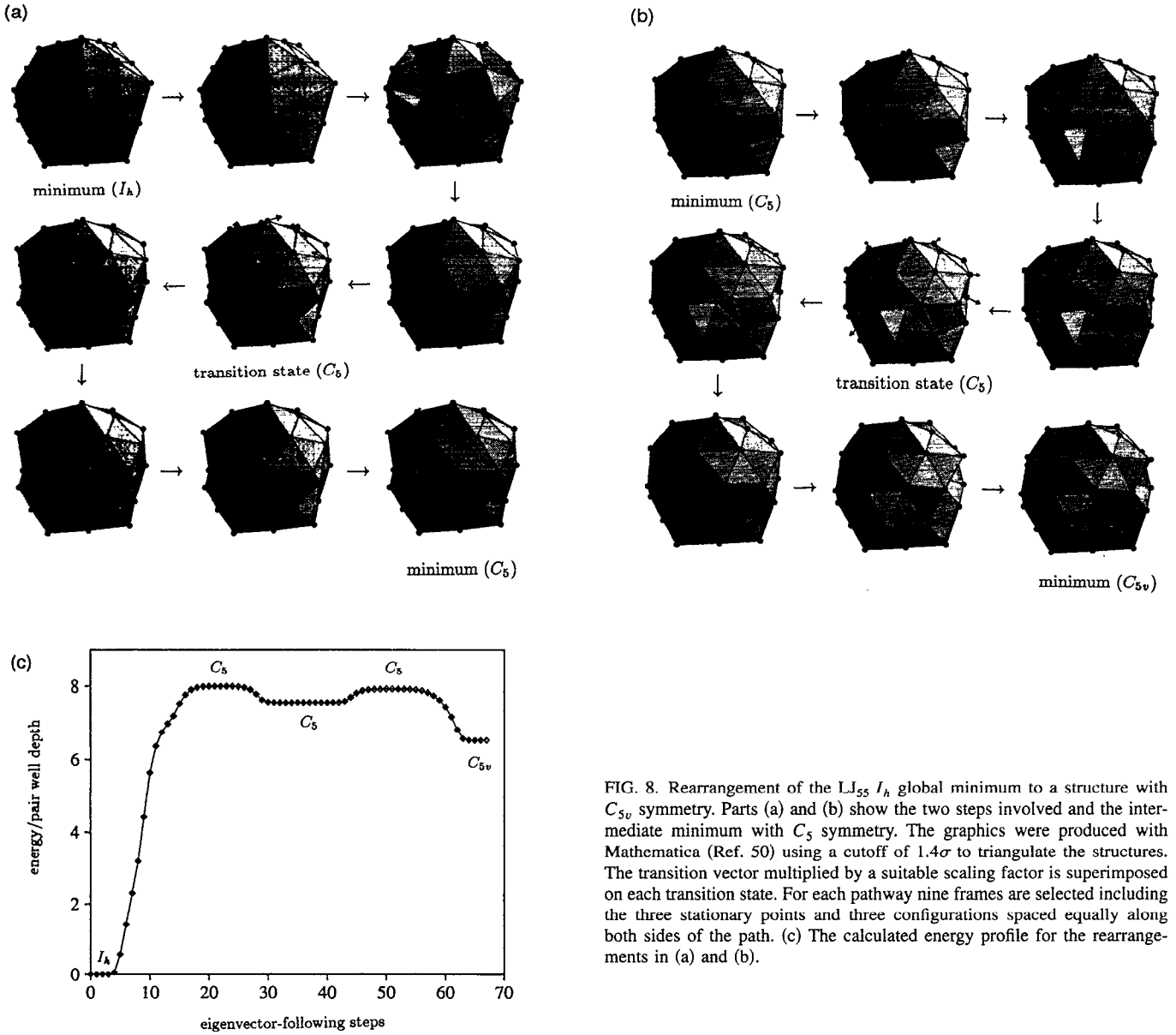

FIG. 8. Rearrangement of the LJ_{55} I_h global minimum to a structure with C_{5v} symmetry. Parts (a) and (b) show the two steps involved and the intermediate minimum with C_5 symmetry. The graphics were produced with Mathematica (Ref. 50) using a cutoff of 1.4σ to triangulate the structures. The transition vector multiplied by a suitable scaling factor is superimposed on each transition state. For each pathway nine frames are selected including the three stationary points and three configurations spaced equally along both sides of the path. (c) The calculated energy profile for the rearrangements in (a) and (b).

we would expect from the variation of W_6 with potential energy in Fig. 9(d). The behavior in the 13 atom cluster is more unusual. The value of W_6 seems to change sign. This may be due to the presence of low-lying energy minima with positive values of W_6 in the 13 atom cluster configurations.

From these calculations we can see that it is not surprising that, of the bond-order parameters, W_6 was the best discriminator between solid and liquidlike phases in our free energy plots for the 55 atom cluster.

C. Calculation of $F(Q)$ from the potential energy surface

In previous work[29] one of us has shown how thermodynamic functions can be calculated, approximately, from the distribution of minima on the potential energy surface (and their normal mode frequencies). The method is based upon the harmonic approximation which gives the expression for the total energy density of states appropriate for the potential well associated with a minimum at energy E^0 as[37]

$$\Omega(E)=\frac{(E-E^0)^{\kappa-1}}{\Gamma(\kappa)\Pi_{j=1}^{\kappa}\nu_j}. \tag{36}$$

We now make the superposition approximation[29] that the total density of states for a multiminima surface is obtained by summing over all the different minima that are low enough in energy to contribute

$$\Omega(E)=\sum_{E_s^0<E}\frac{n_s^*(E-E_s^0)^{\kappa-1}}{\Gamma(\kappa)\Pi_{j=1}^{\kappa}h\nu_j^s}, \tag{37}$$

where n_s^* is the number of distinct permutational isomers of minimum s, i.e., $n_s^* = 2n!/h_s$, and h_s is the order of the point group of s, which was also calculated for all the minima and transition states. Note that Planck's constant has

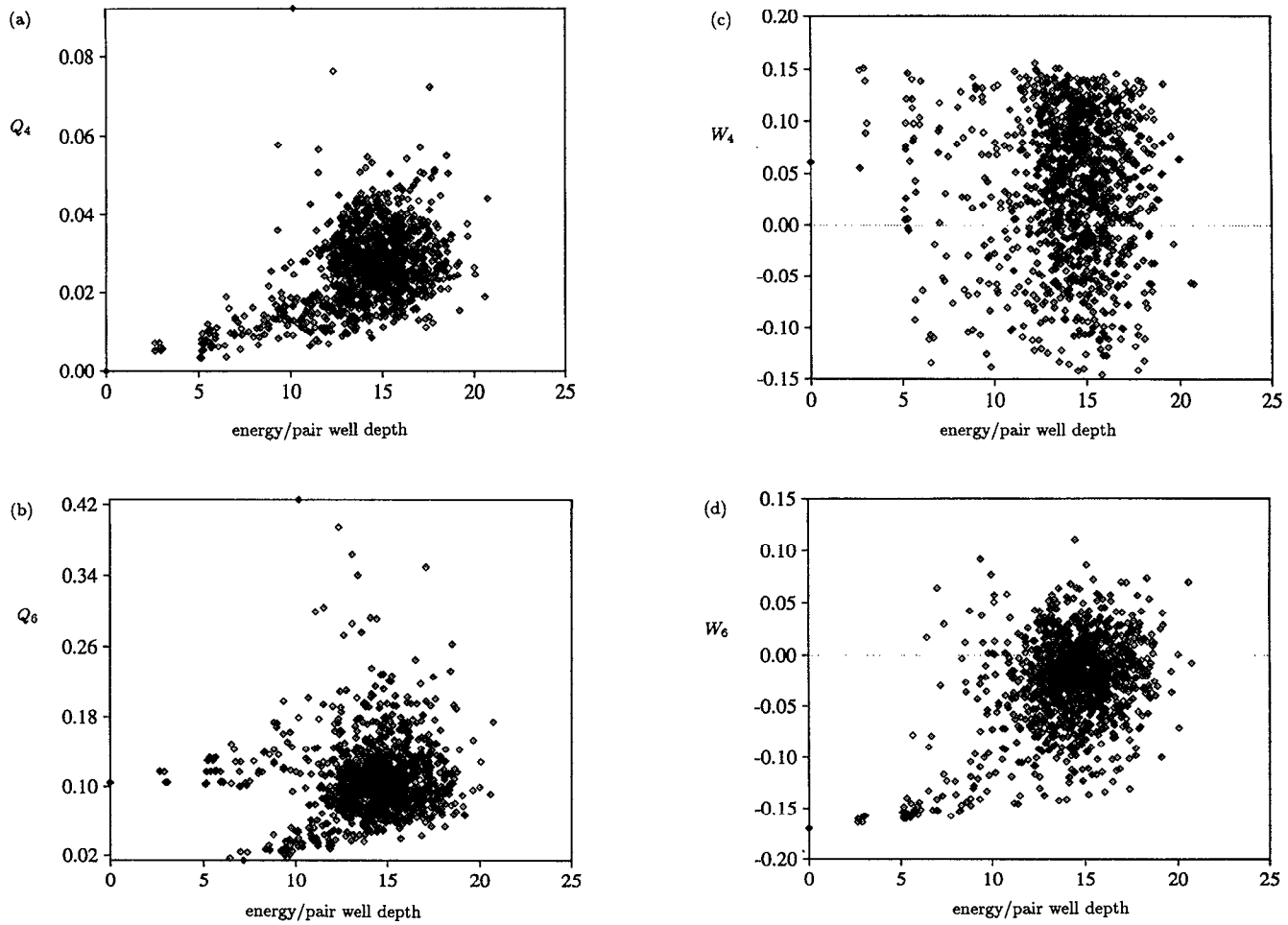

FIG. 9. Scatter plots of the order parameter vs potential energy for local minima of LJ_{55}.

been included in the above expression to convert it to the classical limit of the quantum density of states. A further modification of the above formula employs a substitution in terms of the relative quench probabilities to the different minima. This probably gives better results for larger systems such as LJ_{55} because it provides a better idea of the distribution of minima,[9,29] but we will not make use of it here. A practical problem which may introduce a further error is that we actually have a representative rather than exhaustive sample of minima.

The final expression for the Helmholtz free energy in the harmonic superposition approximation is[9]

TABLE III. Observed values of order parameters.

	System	T^*	$\langle Q_4 \rangle$	$\langle Q_6 \rangle$	$\langle W_6 \rangle$	$\langle$Bonds$\rangle$	$\langle E_c \rangle$
13	Ideal	0	0.0002	0.0415	−0.1698	6.46	0.0
	Solid	0.23	0.046	0.14	0.03	6.11	5.10
	Liquid	0.33	0.10	0.237	0.011	5.28	10.58
55	Ideal	0	0.0006	0.104	−0.1697	8.51	0.0
	Solid	0.27	0.017	0.120	−0.107	8.32	26.0
	Liquid	0.33	0.042	0.116	−0.008	7.47	53.2
147	Ideal	0	0.0002	0.136	−0.1697	9.47	0.0
	Solid	0.33	0.011	0.134	−0.150		
	Liquid	0.39	0.027	0.094	−0.0019		
Bulk	fcc	0	0.191	0.575	−0.013	12	0.0
Local	icosahedral	0	0.0	0.663	−0.1698		

$$A(T)=E_0^0-\frac{1}{\beta}\ln\sum_s \frac{n_s^* e^{-\beta(E_s^0-E_0^0)}}{\Pi_{j=1}^{\kappa}\beta h\nu_j^s}. \tag{38}$$

It may be helpful to compare this expression with the expected result for the more familiar case of equilibrium between m distinct isomers in a canonical ensemble. Let the number of copies of the cluster in the ensemble be n, with n_1 clusters present as isomer (minimum) 1, n_2 as isomer 2, etc. The total free energy for a nonlocalized system is

$$A=-kT\sum_{i=1}^{m}\ln(Z_i^{n_i}/n_i!)=-kT\sum_{i=1}^{m}n_i\ln(Z_i e/n_i), \tag{39}$$

where Z_i is the partition function for a single cluster of type i referred to a common energy zero. Hence we have a sum of logs, rather than the log of a sum as in Eq. (38). However, minimizing A with respect to the n_i subject to the constraint $\Sigma_{i=1}^{m}n_i=n$ gives the familiar result

$$\frac{n_i}{n}=\frac{Z_i}{\Sigma_{j=1}^{m}Z_j}, \tag{40}$$

and hence

$$A=-nkT\ln\left(e\sum_{i=1}^{m}Z_i/n\right). \tag{41}$$

Therefore the superposition approximation, which leads to the log of a sum over minima, gives the same result for the free energy (and other thermodynamic properties) as we would obtain by considering the equilibrium distribution of isomers. The global view of the surface therefore coincides with the more usual view in terms of isomeric equilibrium.

We can exploit the superposition approximation to estimate the Landau free energy, $F(Q)$. If Q is a bond order parameter this can only be done very crudely because the dependence of E_c on Q is complex. However, if we assume that the order parameters remain constant within the potential well associated with a given minimum, s, and equal to the value at that stationary point, then we obtain $F(Q_s)$ from

$$F(Q_s)=E_0^0-\frac{1}{\beta}\ln\frac{n_s^* e^{-\beta(E_s^0-E_0^0)}}{\Pi_{j=1}^{\kappa}\beta h\nu_j^s}. \tag{42}$$

A continuous $F(Q)$ could then be obtained by interpolation. However, this procedure involves major additional approximations which are unnecessary if the order parameter is the potential energy, E_c. Since E_c actually performs better than the bond order parameters in practice we will describe this approach in more detail.

An expression for $F(E_c)$ may be obtained if we delay integration over E_c in the convolution integral for $\Omega(E)$,

$$\Omega(E)=\int_{E^0}^{E}\frac{(E_c-E^0)^{\kappa/2-1}(E-E_c)^{\kappa/2-1}}{\Gamma(\kappa/2)^2\Pi_{j=1}^{\kappa}\nu_j}dE_c. \tag{43}$$

Taking the Laplace transform with respect to E gives

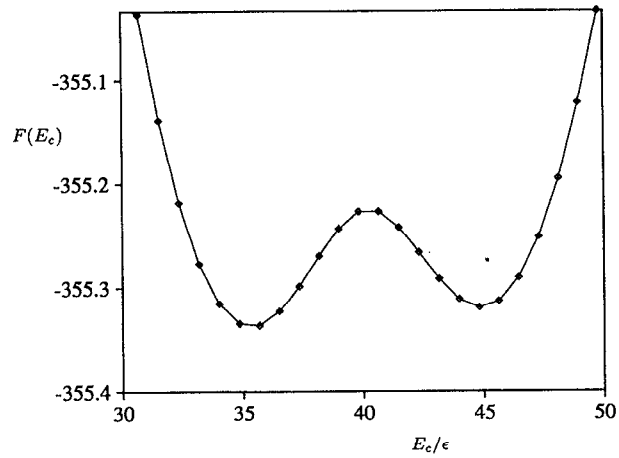

FIG. 10. Variation of the Landau free energy for LJ_{55} as a function of potential energy, E_c, (relative to the global minimum) calculated using a harmonic superposition approximation at $T^*=0.415$ from a sample of 1191 minima obtained in previous work (Ref. 29).

$$Z(\beta)=\int_{E=0}^{\infty}\int_{E_c=E^0}^{E}\frac{(E_c-E^0)^{\kappa/2-1}(E-E_c)^{\kappa/2-1}}{\Gamma(\kappa/2)^2\Pi_{j=1}^{\kappa}\nu_j}\times e^{-\beta E}dE_c\,dE. \tag{44}$$

Interchanging the order and integrating with respect to E after modifying the limits appropriately we find

$$Z(\beta)=\int_{E_c=E^0}^{\infty}\frac{(E_c-E^0)^{\kappa/2-1}}{\Gamma(\kappa/2)\beta^{\kappa/2}\Pi_{j=1}^{\kappa}\nu_j}e^{-\beta E_c}dE_c, \tag{45}$$

and hence, summing over minima and introducing Planck's constant as above,

$$A(\beta)=-kT\ln\sum_s n_s^*\int_{E_c=E_s^0}^{\infty}\frac{(E_c-E_s^0)^{\kappa/2-1}}{\Gamma(\kappa/2)\beta^{\kappa/2}\Pi_{j=1}^{\kappa}h\nu_j^s}\times e^{-\beta E_c}dE_c. \tag{46}$$

The definition of $F(Q)$ now gives

$$F(E_c)=-kT\ln\sum_{E_s>E_c}n_s^*\frac{(E_c-E_s^0)^{\kappa/2-1}}{\Gamma(\kappa/2)\beta^{\kappa/2}\Pi_{j=1}^{\kappa}h\nu_j^s}e^{-\beta E_c}. \tag{47}$$

Although this particular formulation of the superposition model involves significant approximations, particularly the harmonic assumption, the resulting curves do appear to show qualitatively correct features. A double minimum in $F(E_c)$ is found for a narrow temperature range around $T^*=0.41$, i.e., significantly higher than in the simulations, with a barrier height of order 0.1ϵ (Fig. 10).

VI. RESULTS FOR 13 AND 147 ATOM CLUSTERS

Figure 11 shows Landau free energy curves for a 13 atom cluster using the potential energy as the order parameter. Although there is a fairly sharp change in the energy of the minimum between $T^*=0.23$ and 0.33, and we find a shoulder in the free energy at $T^*=0.29$, we have not found a true double minimum. Hence there does not appear to be a

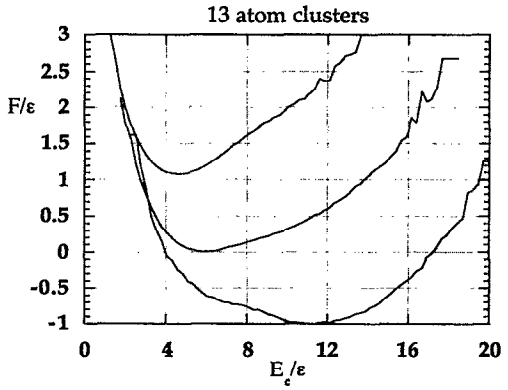

FIG. 11. Variation of the Landau free energy for LJ_{13} as a function of potential energy, E_c, at temperatures (from top to bottom) $T^*=0.23$, 0.29, and 0.33. The choice of the zero of free energy at each temperature is arbitrary.

free energy barrier between the two phases, although the short time averaged temperature in this system exhibits clear bimodality.[5,25,26] This is consistent with the fact that the microcanonical caloric curves for LJ_{13} clusters show an inflection rather than an S-bend.[23]

Figure 12 shows the Landau free energy curves of a cluster of 147 atoms at $T^*=0.37$ which was chosen as the temperature corresponding to the maximum in the specific heat anomaly found by Labastie and Whetten.[2] The order parameter used was a combination of the potential energy and a triple bond-order parameter

$$Q=V/100\epsilon+4W_6, \tag{48}$$

which we found gave a smooth passage over the barrier for this cluster using the biased Monte Carlo method. The height of the barrier between the solid and the liquid phases of this cluster is approximately $1.2-1.5\epsilon$ while that observed in the 55 atom cluster was approximately $0.4-0.5\epsilon$. This variation is consistent with a linear dependence on the number of particles in the cluster. In large enough clusters one would expect the transformation to proceed by the growth of one phase within the other. The barrier would then depend on the

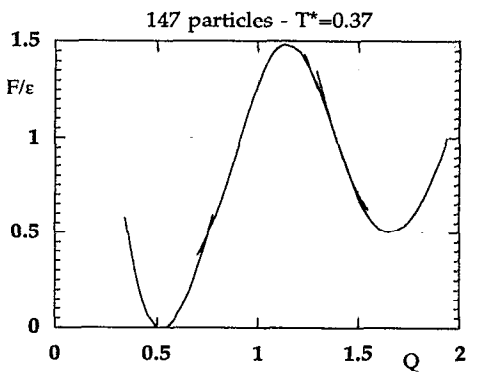

FIG. 12. Variation of the Landau free energy for LJ_{147} with order parameter Q (defined in the text) at $T^*=0.37$. The free energy zero has been chosen at the bottom of the solid well.

total surface free energy of the interface between the phases when the system was half-solid and half-liquid, which would lead to an $N^{2/3}$ dependence. In clusters of the size we are investigating the transformation process involves the whole of the cluster, which leads one to expect the barrier to be approximately proportional to N.

VII. DISCUSSION

The thermodynamics of finite systems has been studied for several decades,[38,39] both by simulations, which really began in the early 1970s, and by analytic theories, which are still being developed. The most recent simulations extract the density of states and use this to calculate various thermodynamic properties.[2,10,40–42] This approach has produced the clearest picture of the solidlike/liquidlike coexistence phenomenon and provided support for previous theoretical conjectures.

The first theory to suggest the existence of distinct stability limits for the solidlike and liquidlike forms of a finite system was based upon a quantum density of states approach.[43–45] However, since the phenomenon in question is found in classical simulations a classical explanation must also be possible, and capillarity theory does indeed predict the existence of a free energy barrier between local minima corresponding to solidlike and liquidlike clusters.[46] The ensemble dependence of thermodynamic results for finite systems was well known to Hill[38,39] and discussed by Honeycutt and Andersen in terms of caloric curves obtained in the canonical and microcanonical ensembles for a range of cluster sizes.[47] Other theoretical studies have focused upon the behavior of model partition functions. Bixon and Jortner showed how simple models for the distribution of minima on the potential energy surface and their normal mode spectra could account for the trends seen in simulations.[19] Microcanonical caloric curves have also been successfully fitted by a model partition function that allows for anharmonicity.[48] Calculations based upon the underlying potential energy surface[9,29] have also been reported in the present work. Sufficient conditions for van der Waals loops or S-bends to arise in finite systems may also be deduced from models based upon a defective lattice.[21,22] The necessary conditions have now been derived too.[23]

Another approach to the cluster coexistence problem, which has been popularized by Berry and co-workers,[1,20] is the use of short time averages of the temperature, particularly in molecular dynamics studies.[49] Bimodal probability distributions of such averages have been interpreted in terms of solidlike and liquidlike regions of the potential energy surface, for which characteristic values of the temperature are manifested over intervals as short as a few vibrational periods. However, relating short time averages to thermodynamic properties is not trivial, and to emphasize this the presence of such bimodality has been termed "time-scale coexistence" in previous work,[29] in contrast to the presence of S-bends in thermodynamic variables which was termed "thermodynamic coexistence." However, it is not clear that these terms are actually helpful. For example, the thermodynamic averages conducted over molecular dynamics and Monte Carlo trajectories themselves also assume a time

scale, because in the infinite time limit an isolated cluster *in vaccuo* would simply evaporate. Actually, this may be better thought of as a phase space restriction: both the conventional short time and long time averages really apply to a *bound* cluster, as we have emphasized in the present work.

The first theory to predict separate melting and freezing points for a finite system was based upon a quantum density of states correlation from a rigid to nonrigid cluster.[43–45] Presumably one could construct a classical argument in much the same way, and hence we can identify the rigidity parameter used in that work as a kind of order parameter. In fact, as we have seen, it is not easy to find a structural order parameter for these Lennard-Jones clusters, but the potential energy appears to serve us reasonably well because the solidlike and liquidlike parts of the surface happen to be well separated in terms of this quantity. Hence, the present order parameter calculations provide a realisation of the original theory in a very real sense.

Coexistence may also be considered in terms of bimodality in short time averaged temperature distributions.[1,6,20] The latter are generally expected to show up when the lowest potential energy minimum has no low energy rearrangement mechanisms to neighboring potential energy minima available, and where the potential energy minima in question have fairly different energies.[5,6] Hence, although we would certainly expect bimodal short time averaged temperature distributions to be associated with a Landau free energy double minimum for the canonical ensemble, this is not strictly necessary.[23] It might actually be possible to use the short time averaged temperature itself as an order parameter, but we have not yet looked into this. Furthermore, short time averages in the microcanonical ensemble would presumably need to be associated with a double maximum in a Landau entropy. In view of the present work we envisage extending the concept of short time averages to order parameters other than the kinetic or potential energy. This would establish a general connection between equilibrium among different regions of phase space identified by an order parameter and thermodynamic properties such as S-bends.

VIII. CONCLUSIONS

We have shown that it is possible to classify the solid and liquid forms of magic number Lennard-Jones clusters using suitable order parameters. LJ_{55} and LJ_{147} show double minima in the Landau free energy $F(Q)$ over a range of temperatures which we identify as coexistence. The barrier height is approximately proportional to the number of particles. The concept of the Landau free energy belongs to the canonical ensemble. Coexistence has also been associated with the presence of an S-bend in the microcanonical or isopotential caloric curves. We have shown that a double minimum in the Landau free energy expressed as a function of the configurational energy is equivalent to the presence of an S-bend in the isopotential caloric curve. Furthermore, the microcanonical caloric curve will generally exhibit the same features as the isopotential analogue. However, the convolution with the kinetic energy distribution will result in less pronounced features for the former ensemble.

The order parameter description associates free energies with distinct regions of phase space, with the proviso that we must be able to find a characteristic property by which we can distinguish them. If an appropriate order parameter can be found then we can actually determine, for example, the range of temperature for which the double minimum exists, and the barrier involved. The use of order parameters provides additional insight into the thermodynamics of clusters. In fact this approach has already led to a better understanding of the relation between short time averaged properties and S-bends.[23]

We have also shown how the thermodynamics and order parameters of the clusters can be related to the properties of the underlying potential surface and that approximate estimates of thermodynamic quantities can be obtained by applying the harmonic superposition approximation.

ACKNOWLEDGMENTS

We are grateful to Dr. J. van Duijneveldt for the use of his program for determining free energy changes of bulk systems which we adapted for clusters. D.J.W. is a Royal Society University Research Fellow. We thank SERC for computational support (Grant Nos. GR/H/57622 and GR/H/04190).

[1] R. S. Berry, T. C. Beck, H. C. Davis, and J. Jellinek, Adv. Chem. Phys. **70B**, 75 (1988).
[2] P. Labastie and R. L. Whetten, Phys. Rev. Lett. **65**, 1567 (1990).
[3] M. J. Grimson, Chem. Phys. Lett. **195**, 92 (1992).
[4] N. Quirke, J. Molec. Sim. **1**, 249 (1988).
[5] T. L. Beck and R. S. Berry, J. Chem. Phys. **88**, 3910 (1988).
[6] D. J. Wales and R. S. Berry, J. Chem. Phys. **92**, 4283 (1990).
[7] J. P. Rose and R. S. Berry, J. Chem. Phys. **96**, 517 (1992).
[8] J. P. Rose and R. S. Berry, J. Chem. Phys. **98**, 3246 (1993).
[9] D. J. Wales and I. Ohmine, J. Chem. Phys. **98**, 7257 (1993).
[10] C. J. Tsai and K. D. Jordan, J. Chem. Phys. **99**, 6957 (1993).
[11] J. S. van Duijneveldt and D. Frenkel, J. Chem. Phys. **96**, 4655 (1992).
[12] R. M. Lynden-Bell, J. S. van Duijneveldt, and D. Frenkel, Mol. Phys. **80**, 801 (1993).
[13] P. J. Steinhardt, D. R. Nelson, and M. Ronchetti, Phys. Rev. B **281**, 784 (1983).
[14] D. H. Li and J. Jellinek, Z. Phys. D **12**, 177 (1989).
[15] J. Jellinek and D. H. Li, Phys. Rev. Lett. **62**, 241 (1989).
[16] J. Jellinek and D. H. Li, Chem. Phys. Lett. **169**, 380 (1990).
[17] F. H. Stillinger and D. K. Stillinger, J. Chem. Phys. **93**, 6013 (1990).
[18] D. Lynden-Bell and R. M. Lynden-Bell, Mon. Not. R. Astron. Soc. **181**, 405 (1977).
[19] M. Bixon and J. Jortner, J. Chem. Phys. **91**, 1631 (1989).
[20] H. L. Davis, T. L. Beck, P. A. Braier, and R. S. Berry, in *The Time Domain in Surface and Structural Dynamics*, edited by G. J. Long and F. Grandjean (Kluwer Academic, Dordrecht, 1988), p. 535.
[21] R. S. Berry and D. J. Wales, Phys. Rev. Lett. **63**, 1156 (1989).
[22] D. J. Wales and R. S. Berry, J. Chem. Phys. **92**, 4473 (1990).
[23] D. J. Wales and R. S. Berry, Phys. Rev. Lett. (submitted).
[24] D. D. Frantz, D. L. Freeman, and J. D. Doll, J. Chem. Phys. **97**, 5713 (1992).
[25] J. Jellinek, T. L. Beck, and R. S. Berry, J. Chem. Phys. **84**, 2783 (1986).
[26] T. L. Beck, J. Jellinek, and R. S. Berry, J. Chem. Phys. **87**, 545 (1987).
[27] M. P. Allen and D. J. Tildesley, *The Computer Simulation of Liquids* (Clarendon, Oxford, 1987).
[28] D. J. Evans and G. P. Morriss, Phys. Lett. A**98**, 433 (1983).
[29] D. J. Wales, Mol. Phys. **78**, 151 (1993).
[30] S. M. Thompson, K. E. Gubbins, J. P. R. B. Walton, R. A. R. Chantry, and J. E. Rowlinson, J. Chem. Phys. **81**, 530 (1984).
[31] T. A. Weber and F. H. Stillinger, J. Chem. Phys. **80**, 438 (1984).
[32] F. H. Stillinger and T. A. Weber, J. Chem. Phys. **81**, 5089 (1984).

[33] D. J. Wales, J. Chem. Soc. Faraday Trans. **89**, 1305 (1993).
[34] A. C. Mackay, Acta. Crystallogr. **15**, 916 (1962).
[35] D. J. Wales, Chem. Phys. Lett. **166**, 419 (1990).
[36] D. J. Wales, J. Chem. Soc. Faraday Trans. **88**, 653 (1992).
[37] F. G. Amar and R. S. Berry, J. Chem. Phys. **85**, 5943 (1986).
[38] T. L. Hill, *The Thermodynamics of Small Systems Part I* (Benjamin, New York, 1963).
[39] T. L. Hill, *The Thermodynamics of Small Systems Part II* (Benjamin, New York, 1964).
[40] H. P. Cheng, X. Li, R. L. Whetten, and R. S. Berry, Phys. Rev. A **46**, 791 (1992).
[41] H.-P. Cheng and R. S. Berry, Phys. Rev. A **45**, 7969 (1992).
[42] S. Weerasinghe and F. G. Amar, J. Chem. Phys. **98**, 4967 (1993).
[43] G. Natanson, F. Amar, and R. S. Berry, J. Chem. Phys. **78**, 399 (1983).
[44] R. S. Berry, J. Jellinek, and G. Natanson, Phys. Rev. A **30**, 7241 (1984).
[45] R. S. Berry, J. Jellinek, and G. Natanson, Chem. Phys. Lett. **107**, 227 (1984).
[46] H. Reiss, P. Mirabel, and R. L. Whetten, J. Phys. Chem. **92**, 7241 (1988).
[47] J. D. Honeycutt and H. C. Andersen, J. Phys. Chem. **91**, 4590 (1987).
[48] S. F. Chekmarev and I. H. Umirzakov, Z. Phys. D **26**, 373 (1993).
[49] C. L. Briant and J. J. Burton, J. Chem. Phys. **63**, 2045 (1975).
[50] S. Wolfram, *Mathematica* (Addison-Wesley, Redwood City, 1991), 2nd ed.